Matching 3D Lung Surfaces with the Shape Context Approach

2 authors:

Martin Urschler
Ludwig Boltzmann Institute for Clinical-Fore…
101 PUBLICATIONS **915** CITATIONS

Horst Bischof
Graz University of Technology
766 PUBLICATIONS **20,324** CITATIONS

Some of the authors of this publication are also working on these related projects:

Project Automatic age estimation from skeletal and dental MRI data using machine learning View project

Project Nonlinear intra-modality registration View project

Matching 3D Lung Surfaces with the Shape Context Approach.[1]

Martin Urschler, Horst Bischof

Institute for Computer Graphics and Vision, TU Graz

Inffeldgasse 16, A-8010 Graz

E-Mail: {urschler, bischof}@icg.tu-graz.ac.at

Abstract:

Studying the complex thorax breathing motion is an important research topic for medical (e.g. fusion of function and anatomy, radiotherapy planning) and engineering (reduction of motion artifacts) questions. In this paper we present first results on investigating the 4D motion of segmented lung surfaces from CT scans at several different breathing states. For this registration task we extend the shape context approach for shape matching by Belongie et al. [2] from 2D shapes to 3D surfaces and apply it to segmented lung data. Resulting point correspondences can be used e.g. for non-rigid thin-plate-spline registration. We describe our experiments on phantom and real thorax data and show our promising results.

1 Introduction

According to the European Respiratory Society, lung diseases rank second behind cardiac diseases in terms of mortality and cost of treatment. Predictions for the next decade show further rises in lung cancer and respiratory illnesses. Computerized methods for objective, accurate and reproducible analysis of lung structure and function can provide important insights into these problems. However, due to the complexity of the breathing motion, investigations are often very complicated.

In this paper we present first results on studying the 4D motion of segmented lung surfaces from several different breathing states scanned between Functional Residual Capacity (FRC) and Total Lung Capacity (TLC). We especially regard the problem of matching surfaces from consecutive breathing states and non-rigidly registering them by performing a thin-plate spline transform on the corresponding points. In general it is not possible to robustly derive corresponding features from the lung surface since the diaphragm-induced motion component and the movement of the rib cage, where the lung is attached to by adhesive forces, tend to

---

deform the elastic lung tissue, such that e.g. ridges might become valleys.

The shape context approach introduced by Belongie et al. [2] was reported as a reasonable and promising method for matching 2D shapes (especially hand-written digits and letters) and 2D object recognition without relying on extracted features. We extend this approach to match 3D shapes and we are up to our knowledge the first ones to apply it to 4D medical image data, i.e. the segmented lung surfaces at several breathing states.

Our image data stems from a high-speed multi-detector spiral CT. The data is acquired at several (two, four or five) breathing states between TLC and FRC by a protocol where breath is held at fixed inspiration levels during the 30 sec scan time. This leads to a static breathing scheme, which has to be considered for the interpretation of derived motion models from matched and registered shapes. However, a protocol to scan thorax anatomy at different breathing states with high spatial resolution during dynamic (normal) breathing is currently not feasible. The image dimensions per breathing state are 512x512x500 with voxel dimensions of 0.52mm x 0.52mm x 0.6mm.

2 Methods

2.1 Related Work

An older survey on the state of the art in 2D shape matching can be found in Veltkamp et al. [9]. Audette et al. give an algorithmic overview of surface registration techniques for medical imaging in [1], while Zitova et al. recently published an overview of image registration techniques [10]. Some examples for closely related methods for shape matching/registration are Iterative Closest Point techniques [3] the modal matching approach proposed by Sclaroff et al. [8] or the TPS-RPM (Thin-Plate Spline - Robust Point Matching) method developed by Chui et al. [6]. The main contribution of the work from Belongie et al. [2] is to present a robust and simple algorithm for finding shape correspondences by using shape context as a very discriminative representation that incorporates global shape information into a local descriptor.

2.2 The Shape Context Approach

The shape context approach treats objects as (possibly infinite) point sets and assumes that the shape of an object is captured by a finite subset of its points, giving us a set $P = \{p_1, ..., p_n\}$. The points can be obtained as locations of edges from an edge detector or from another method to sample contour/surface points from a shape. The points need not and typically will not correspond to key points or structures such as maxima of curvature, inflection points or surface ridges. In contrast to the original implementation we lay strong emphasis on the discretization

method. We are using a marching-cubes polygonization and sample contour points regularly from the constructed mesh. For each point p_i on the first shape, the "best" matching point q_i on the second shape has to be located. Therefore the shape context descriptor is introduced. If we look at the set of vectors emitted from one point to all others, we can interpret this set as a rich description of the shape configuration relative to that point. Since this description is much too detailed, we take the distribution of the set of vectors as a compact, yet highly discriminative descriptor instead. So for each point p_i a histogram h_i of the relative position of the remaining points is calculated which is called the *shape context*. Now for point p_i from the first shape and q_j from the second shape, let $C_{ij} = C(p_i, q_j) = \frac{1}{2} \sum_{k=1}^{K} \frac{[h_i(k) - h_j(k)]^2}{h_i(k) + h_j(k)}$ denote the cost of matching these two points. Given the set of costs C_{ij} between all pairs of points on the first and second shape, we want to minimize the total cost of this one-to-one matching problem, which is an instance of the weighted bipartite matching problem. It can be solved in $O(N * (M + N * logN))$ time, with N being the number of nodes and M the number of edges in the graph. Here the original matching algorithm has been replaced by a more efficient one since the 3D case requires many more sample points than the 2D case which may lead to high run-times of the algorithm. The result of this step is a one-to-one mapping of corresponding points from the two shapes.

2.3 Non-rigid Registration

Although we do not go into detail on registering the lung surfaces in this paper, it should be mentioned that for the purpose of non-rigid registration of the corresponding point sets we use a thin-plate-spline approach [5] due to its good applicability for modeling changes in biological forms.

3 Experiments & Results

3.1 Preprocessing

From our CT image data of the thorax we first of all have to segment the lung surfaces. This is performed by a simple region-growing algorithm with an increasing threshold interval [4]. The seed point of the region growing algorithm is located in the airway tree (trachea) of the topmost image. The region grower reports a certain number of segmented voxels for each threshold interval. When looking at the curve created by plotting the number of segmented voxels over the threshold levels, there are two characteristic points where the curves' gradient magnitude changes, first for an airway segmentation that starts to leak into the lung tissue and second for a lung segmentation starting to leak into the tissue surrounding the lungs. By taking the region grow result according to this second threshold level we get an accurate lung segmentation. Finally the result is morphologically closed to remove small vessel structures.
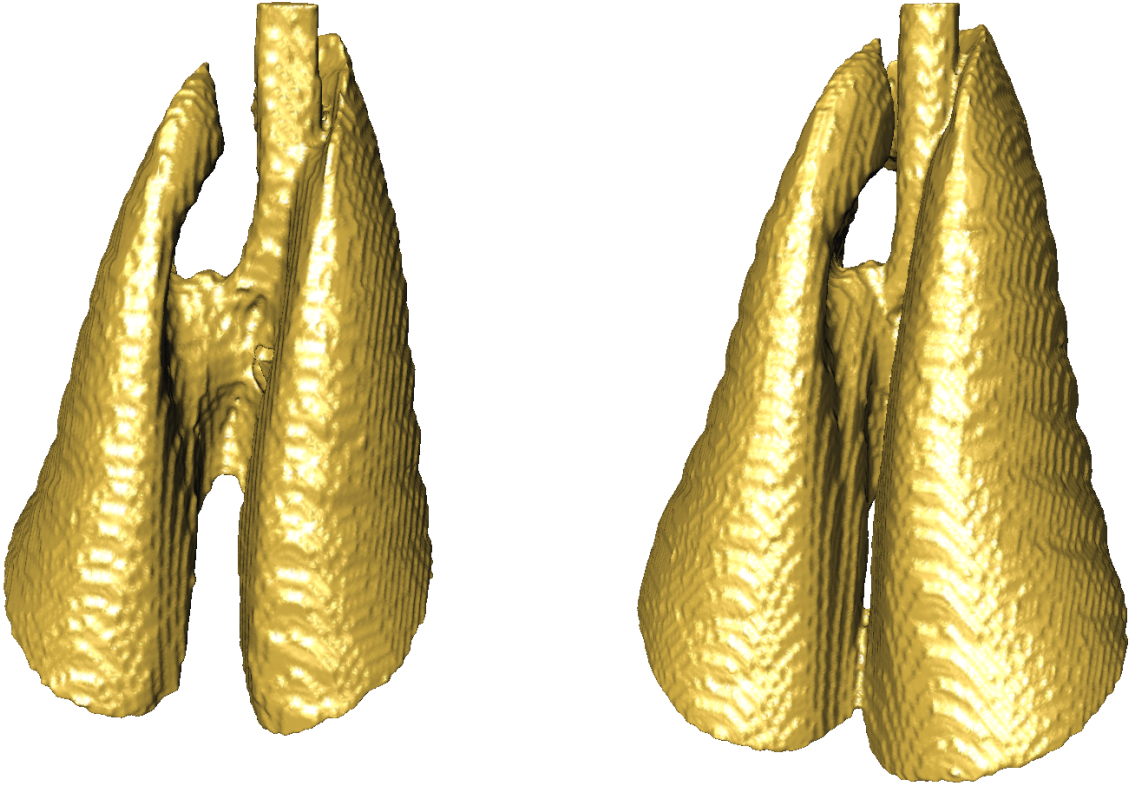
Figure 1: An example for segmented lung surfaces. The left image shows the lung at Functional Residual Capacity (FRC), the right one at Total Lung Capacity(TLC).

We have to note on this simple algorithm that it works very well on our high-resolution, low SNR (due to a high dose) non-pathological sheep study images, while the extracted lung surfaces from lower quality or pathological image data would be a little worse, demanding a more sophisticated algorithm for lung surface segmentation. Fig. 1 shows an example for segmented lung surfaces at FRC and TLC respectively, visualized by using a polygonal mesh representation created with the Simplex Mesh algorithm [7].

3.2 Experiments

We performed several kinds of experiments with the shape context approach. First we used some simple shapes and tried to match them with themselves to show the basic validity of the shape context implementation. The algorithm found all corresponding points as expected. Second we created a phantom box-like shape and deformed it slightly by a known transformation in analogy to inflating a balloon. More specifically we determined the center point of the point set and applied a radial translation of each point from the center point in the direction of the vector between point and center. The magnitude of the translation was determined as 0.2 times the distance between point and center. For the box shape we sampled 1000 points from three of the six faces. The shape matching algorithm was able to find all correspondences correctly, a fact that was proven by inverting the known transformation. The matching result
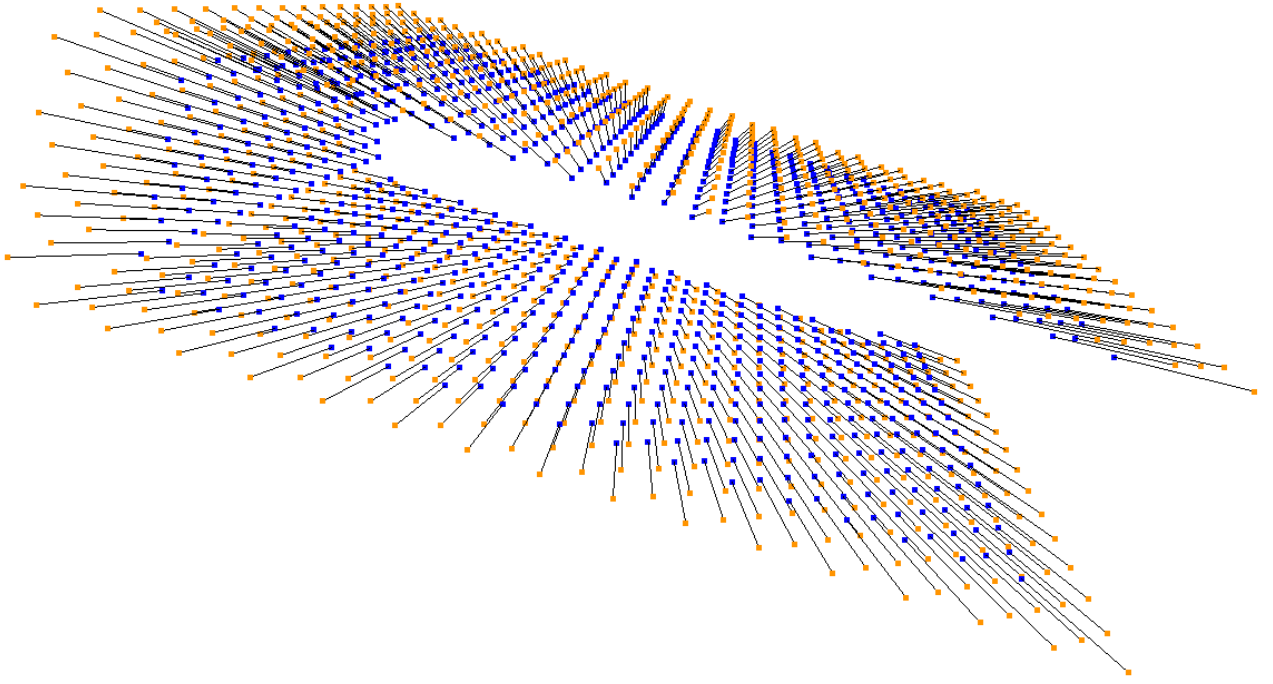
Figure 2: A simple phantom box shape and its transformed (inflated) counter part. The dark lines show the correspondences between the 1000 sample points.

is shown in Fig. 2.

Another experiment involved the same procedure described above, yet we applied it on a lung surface segmentation result. Using a balloon-like force to virtually inflate a given lung surface has the advantage of being simple to implement but still approximating the real lung behaviour in a certain way. Again we were able to evaluate the correspondences by inverting the known transformation and transforming the matched 100 and 1000 sample points respectively back to the ground-truth point set. The shape matching approach resulted in 100 and accordingly 1000 correct matches as illustrated in Fig. 3.

In the last experiment we matched segmented real-life lung surfaces at Total Lung Capacity and Functional Residual Capacity and validated the results visually in a first step. The results of this step are shown in Fig. 4 for 300, 1000 and 2000 sample points respectively. The visual examination of the result shows an excellent correspondence of the matched surfaces. The matching lines clearly show that there is a breathing-like form of non-rigid transformation waiting to be derived in a following registration step. For further evaluation of the real data we will use our data sets with 5 distinct breathing states, find correspondences between state 1 and 3 and state 3 and 5, derive the non-rigid registration using a thin-plate spline model and compare the warped and interpolated surfaces with the given states 2 and 4.
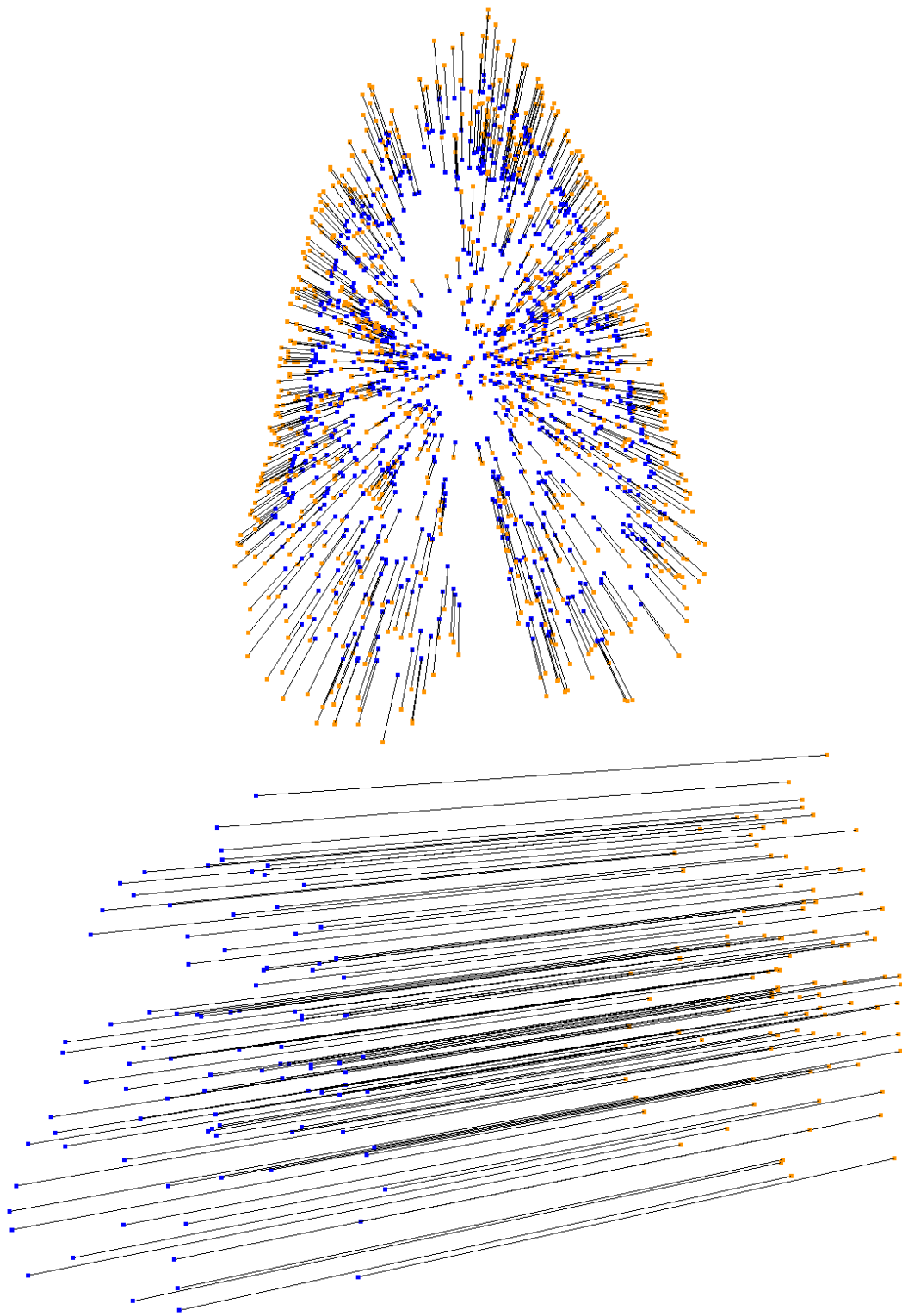
Figure 3: A lung surface shape and its transformed (inflated) counter part. Sampled with 1000 points in the upper image and with 100 points in the lower image The dark lines show the correspondences.

4 Discussion & Future Work

In this paper we presented an extension of the shape context approach for shape matching of 3D lung surfaces. The shape context approach is a very promising technique to prepare non-rigid registration of deformable anatomical structures. Our first experiments showed an excellent performance on the phantom data and promising results on real data, with more validations being in preparation.

Further work will be performed on the shape discretization issue, where we intend to use simplex meshes for polygonization instead of the marching cubes algorithm. Another issue is the graph matching algorithm where we will investigate a more efficient heuristic approach that reduces the amount of regarded graph edges thereby reducing the algorithms run-time from $O(N * (M + N * logN))$ to $O(N^2 * logN)$. The third issue is the already mentioned technique for validation of the real-life data by using a data set with 5 distinct breathing states and trying to explain 2 of the 5 states by matching, registration and warping.

References

[1] M. A. Audette, F. P. Ferrie, and T. M. Peters. An algorithmic overview of surface registration techniques for medical imaging. *Medical Image Analysis*, 4:201–217, 2000.

[2] S. Belongie, J. Malik, and J. Puzicha. Shape matching and object recognition using shape contexts. *IEEE Transactions on Pattern Analysis and Machine Intelligence*, 24(4):509–522, 2002.

[3] P. J. Besl and N. D. McKay. A method for registration of 3-D shapes. *IEEE Transactions on Pattern Analysis and Machine Intelligence*, 14(2):239–256, 1992.

[4] D. Boehm, S. Krass, A. Kriete, W. Rau, D. Selle, H.-H. Jend, and H.-O. Peitgen. Segmentbestimmung im Computertomogramm der Lunge. In *Bildverarbeitung fuer die Medizin*, pages 168–172, Berlin, 2000. Springer.

[5] Fred L. Bookstein. Principal Warps: Thin-Plate Splines and the Decomposition of Deformations. *IEEE Transactions on Pattern Analysis and Machine Intelligence*, 11(6):567–585, June 1989.

[6] H. Chui and A. Rangarajan. A new point matching algorithm for non-rigid registration. *Journal of Computer Vision and Image Understanding*, 89:114–141, 2003.

[7] H. Delingette. Simplex Meshes: A General Representation for 3D Shape Reconstruction. Technical Report 2214, Unite de recherche INRIA Sophia-Antipolis - Projet Epidaure, March 1994.

[8] S. Sclaroff and A. Pentland. Modal Matching for Correspondence and Recognition. *IEEE Transactions on Pattern Analysis and Machine Intelligence*, 17(6):545–561, June 1995.

[9] R. C. Veltkamp and M. Hagedoorn. State of the Art in Shape Matching. Technical Report UU-CS-1999-27, Utrecht, 1999.

[10] B. Zitova and J. Flusser. Image registration methods: A survey. *Image and Vision Computing*, 21(11):977–1000, October 2003.
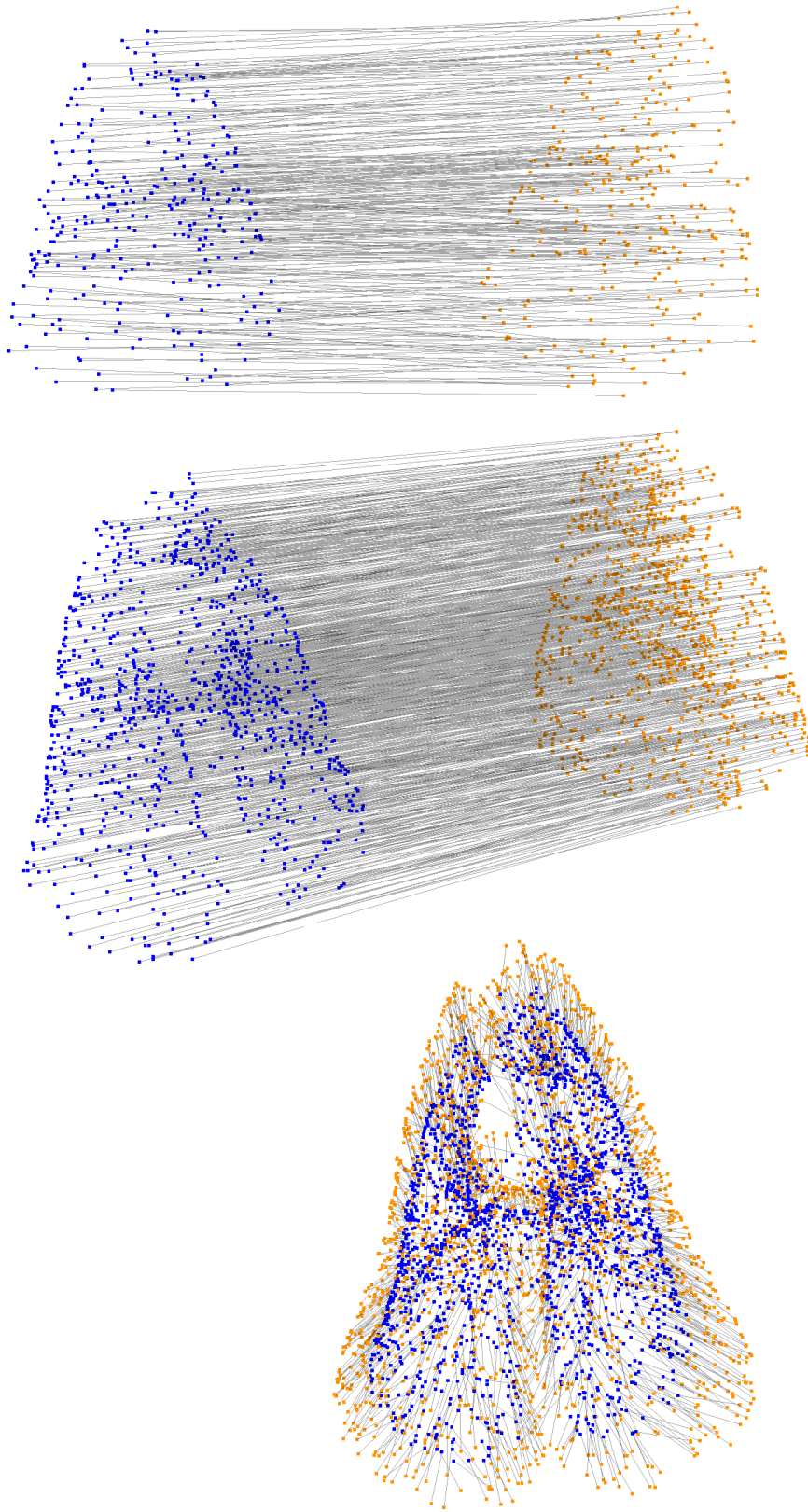
Figure 4: Shape matching result from real life data taken at Functional Residual Capacity and Total Lung Capacity respectively. Top image shows matching result with 300, middle image 1000 and bottom image 2000 sampled points. The dark lines show the correspondences.